JBC Papers in Press. Published on December 16, 2016 as Manuscript M116.766964
The latest version is at http://www.jbc.org/cgi/doi/10.1074/jbc.M116.766964

Barbiturates bind in the GLIC ion channel pore and cause inhibition by stabilizing a closed state

‡Zaineb Fourati (1), ‡Reinis Reinholds Ruza (1), ‡Duncan Laverty (2), Emmanuelle Drège (3), Sandrine Delarue-Cochin (3), Delphine Joseph (3), Patrice Koehl (4), *Trevor Smart (2) and *Marc Delarue (1)

1. Unité de Dynamique Structurale des Macromolécules, UMR 3528 du CNRS, Institut Pasteur, 75015 Paris, France

2. Department of Neuroscience, Physiology and Pharmacology, University College London, London, WC1E 6BT, UK

3. UMR 8076 du CNRS, BioCIS, Faculté de Pharmacie, Université Paris Sud, 92296 Chatenay-Malabry, France

4. Department of Computer Science, UC Davis, Davis, CA 95616, USA

‡ These authors should be considered as co-first authors

delarue@pasteur.fr

Keywords: x-ray crystallography, ligand-gated ion channels, barbiturates

Running title: Barbiturates bind a closed state in the pore of cationic pLGICs

ABSTRACT: Barbiturates induce anesthesia by modulating the activity of anionic and cationic pentameric ligand-gated ion channels (pLGICs). Despite more than a century of use in clinical practice, the prototypic binding site for this class of drugs within pLGICs is yet to be described. In this study, we present the first X-ray structures of barbiturates bound to GLIC, a cationic prokaryotic pLGIC with excellent structural homology to other relevant channels sensitive to general anesthetics and, as shown here, to barbiturates, at clinically-relevant concentrations. Several derivatives of barbiturates containing anomalous scatterers were synthesized and helped to unambiguously identify a unique barbiturate binding site within the central ion channel pore in a closed conformation. In addition, docking calculations around the observed binding site for all three states of the receptor, including a model of the desensitized state, showed that barbiturates preferentially stabilize the closed state. The identification of this pore binding site sheds light on the mechanism of barbiturates inhibition of cationic pLGICs and allows the rationalisation of several structural and functional features previously observed for barbiturates.

INTRODUCTION

The arrival of the first barbiturates into clinical practice at the beginning of the 20th century caused a revolution in the pharmacology-based treatments of psychiatric and neurological disorders due to their sedative and anxiolytic properties [1]. As anticonvulsants, barbiturates were responsible for the first truly effective management regimens for epileptic seizures, while in the field of general anaesthesia they were the first injectable agents used for induction. Between 1920 and 1950 barbiturates were the most prominent class of drugs used as sedatives and hypnotics [2]. As they are prone to cause respiratory depression, they have now been mostly replaced with the comparatively safer benzodiazepines [3]. Despite this, barbiturates still retain several important sedative-hypnotic roles in medical treatment such as for asthmatic and gastrointestinal functional disorders, certain types of epilepsy, violent convulsions and cerebral haemorrhages. Most importantly, they are still used for the induction of general anaesthesia.

Although barbiturates have enjoyed widespread use during the last century, insights into the molecular basis of their action have only arisen during the last couple of decades. Barbiturates are thought to modulate the action of various neural receptors, such as the AMPA/kainate receptors and the P/Q high voltage-activated calcium channels [4,5], as well as members of the pentameric ligand-gated ion channel family, which are major mediators of synaptic transmission [6]. It has been shown that barbiturates alter the action of anionic GABAA and glycine receptors, promoting their activation and subsequent polarisation of neurons [7–9], as well as inhibiting cationic ion channels responsible for triggering interneuronal signalling, such as the nicotinic acetylcholine receptors (nAChRs) and 5HT3Rs [10–12]. Enhancement of GABAAR signalling is thought to be the primary mechanism responsible for the depressant effects of barbiturates [13], although other targets, such as the nAChRs and their inhibition might still play an important role in the overall depression of the nervous system.

Pentameric ligand-gated ion channels are either homo- or heteropentamers in which subunits are arranged laterally around a central axis of symmetry, thus forming the central pore [14]. A single subunit consists of an N-terminal extracellular agonist-binding domain, containing approximately 200 amino acids forming several β-strands arranged in immunoglobulin-like β-sandwich folds, and a transmembrane domain consisting of 4 α-helices, M1-M4. Most of these helices are exposed to the cellular membrane, except for M2 , which lines the central ion channel pore. pLGICs can adopt several conformations, such as the closed, open and desensitised states, which mostly depend on the presence and the length of exposure to agonists [15].

So far, most of the progress on characterising the binding site of barbiturates within both the $GABA_AR$ and the nAChR have been made using binding and photolabelling studies. In the case of cationic nAChRs, such studies have shown that barbiturates bind within the closed or desensitised central ion channel pore, since most of them fully inhibit the binding of channel blockers stabilising the receptors in these states [16], while photoreactive barbiturate derivatives are capable of labelling several residues within the channel pore of receptors in the desensitized state [17]. However, detailed structural characterisation of the barbiturate binding site within pLGICs is still lacking. While crystal structures of barbiturate-bound globular proteins [18] have been determined, there is no evidence that these complexes can inform us on the interactions existing between the ligand and its actual membrane-bound receptor.

To further our knowledge on barbiturate mechanism of action, we used x-ray crystallography to study their binding with the locally-closed form of GLIC – a cationic prokaryotic homologue of pLGICs. GLIC shows remarkable structural homology with the

previously solved *Torpedo marmorata* nAChR structure by electron microscopy [19,20], and shares similar electrophysiological responses to general anaesthetics [21]. In this study, we describe firstly a potent effect of barbiturates on GLIC, as shown by electrophysiology, and then crystal structures at atomic resolution of GLIC-barbiturate complexes. This reveals a binding site for barbiturates in the closed central ion channel pore of cationic pLGICs, thus informing on the molecular basis for inhibition by barbiturates. In addition, we built a model of the desensitised form of GLIC based on the only available structure of a representative D-state in the pLGIC family, namely the GABAA receptor β3 homo-pentamer [22] and performed docking calculations of these ligands on the closed, open and (modelled) desensitised states of GLIC. This allowed us to qualitatively predict the changes in affinity for the observed (pore) binding site in different conformational states of the receptor. The predicted relative affinities suggest a mode of action for barbiturates based upon stabilising the closed conformation of the receptor.

RESULTS

Chemical synthesis of selenocyanobarbital and thiopental

As membrane proteins are usually prone to limited resolution on X-ray crystallography, we used three barbiturate derivatives harboring atoms that produce specific anomalous signal: the commercially available 5-(2-bromo-ethyl)-5-ethyl-pyrimidine-2,4,6-trione that we called "bromobarbital"; thiopental; and selenocyanobarbital, both chemically synthesized in this study. Selenocyanobarbital **6** was synthesized in a five-step sequence (Fig. 1-A). Briefly, dimethyl 2-ethylmalonate **1** was first alkylated in the presence of sodium hydride by 2-(2-bromoethoxy)tetrahydropyran **2**. The latter was previously prepared according to a procedure described in the literature, giving the 2,2-disubstituted malonate **3** in a 47% yield [23]. Then**,** the ω-iodo-barbiturate intermediate **5** was synthesized over three steps: (i) the condensation of urea with malonate **3** in the presence of sodium hydride, followed by (ii) the hydrolysis of the tetrahydropyran ether with p-toluenesulfonic acid in methanol and (iii) the iodination of the resulting alcohol afforded the expected iodinated barbiturate in a 47% yield. The reaction of the iodide 5 with potassium selenocyanate in THF furnished the targeted selenocyanobarbital 6 in a 60% yield.

Due to stock unavailability, thiopental **7** was synthesized in two steps starting from the commercially available pentobarbital sodium salt (Fig. 1-B). The latter was first neutralized with a 1M HCl solution to release the barbituric acid form which was then transformed into thiopental **7** in a modest 20% yield, by using Lawesson reagent in refluxing anisole.

Barbiturates inhibit GLIC at clinically relevant concentrations

To determine if GLIC is sensitive to modulation by barbiturates, we expressed wild-type GLIC channels in *Xenopus* oocytes and characterised the effect of pentobarbital as well as the three barbiturate derivatives using two-electrode voltage clamp electrophysiology. None of the tested barbiturates evoked a direct response at GLIC when applied at neutral pH 7. However, in all cases, when the barbiturates were co-applied in the presence of the orthosteric agonist for GLIC, protons (at pH 5.5, ≈ pEC_{10-20}), a pronounced inhibition of the proton-induced current was observed (Fig. 2A-E). The barbiturate-mediated inhibition was reversible with subsequent applications of pH 5.5 recording solution (in the absence of barbiturate) eliciting undiminished current amplitudes when compared to that obtained prior to drug-application (Fig.2 B-E). The concentration-inhibition curves for pentobarbital and bromobarbital revealed similar inhibitory potencies at GLIC (IC_{50} of 101 ± 4.9 μM and 177 ± 27.2 μM respectively, n = 5 and 6), with near complete inhibition of the proton response at 1-3 mM (Fig. 2-A). By contrast, the inhibition curve for thiopental revealed an approximate 4-fold increase in potency (IC_{50} of 24.4 ± 1.2 μM, n=5), when compared to pentobarbital. Intriguingly, in most recordings at higher concentrations of thiopental (≥ 300 μM), a rebound current was observed upon wash-out of the drug that virtually attained the same amplitude as the control proton-activated current (Fig. 2F).

The micromolar to millimolar concentration range for the barbiturates to modulate GLIC channels is similar to that reported for these compounds to impart their effects at eukaryotic pLGICs [24]. Moreover, it is notable that independent pharmacological screening studies of the related prokaryotic homolog ELIC revealed insensitivity to modulation by pentobarbital [25]. Given the sensitivity of GLIC to pharmacologically-relevant concentrations of a range of barbiturate compounds (Fig 2), we therefore sought to determine whether their mechanism of action utilises a common binding site on GLIC.

Barbiturates bind within the ion channel pore of GLIC

To explore the possibility that barbiturates are binding to the channel in an open state, as shown for other anaesthetic compounds [26], we collected several diffraction data sets of wild-type GLIC crystals at pH 4 (open form) with varying concentrations of three barbiturate derivatives. However we were unable to detect any barbiturate binding in the open receptor. This is in agreement with the inhibitory action of barbiturates on GLIC, which suggests that they should stabilize the closed state. To determine whether binding could be rather observed in the closed state of the receptor, we co-crystallized the different barbiturate compounds with a locally-closed (LC) mutant of GLIC [27]. This mutant has a resting-like conformation in the transmembrane domain where other general anesthetics, such as Xenon or bromoform, were recently found to bind, inside the channel pore (Fig. 3) [28,29].

All three barbiturate derivatives (Fig. 4-A) could be co-crystallized with the locally-closed form of GLIC and diffracted up to 3.5-3.0 Å resolution (Table 1). Strikingly, all barbiturate molecules were observed bound within the central ion pore, between the pore-lining T2' and I9' sidechains (Fig. 4). The main interactions responsible for binding are hydrogen bonds formed between the serines at position 6' and the carbonyl groups of the barbital ring, although van der Waals forces also play a role, with the long aliphatic tails of the barbiturates being further stabilised by either isoleucines or threonines at levels 9' and 2' respectively. No evidence of binding was observed to other sites. The RMSD of the barbiturate bound structures and the apo-protein were small (less than 0.6 Å), with the biggest differences in Cα position being found at the short intracellular loops between helices M3 and M4, as well as at the top of the flexible ECD, both of which participate in crystallographic contacts. The largest value of RMSD was 0.587 Å for the thiopental bound form of GLIC.

The barbiturates used in the crystallisation experiments were a racemic mixture of both enantiomers, therefore diminishing the observability of the aliphatic barbiturate tails. Because of this, their orientation was fitted based mainly on the anomalous peaks of bromine, sulfur or selenium atoms in the bromobarbital, thiopental and selenocyanobarbital derivatives, respectively (Fig. 4).

In Bromobarbital the second carbonyl is positioned between two serine 6' sidechains at approximately equal distances of 2.9 Å and 3.0 Å (Fig. 4-B), thus indicating the existence of hydrogen bonds between them. The closest serine among those two could also participate in a weaker hydrogen bond with the barbiturate ring nitrogen. This also permits the orientation of one of the other barbiturate carbonyl groups 2.7 Å away from the opposite serine 6' and the formation of an additional hydrogen bond (Fig. 4-C). The bromoethane tail is held by van der Waals forces in the proximity of isoleucine sidechains at the level of the 9' ring of M2 residues (Fig. 4-B).

In thiopental the extra methyl group in the isoamyl chain (Fig. 4-A) and the more lipophilic nature of the thiol group as a hydrogen bond acceptor imposes additional restraints on the possible orientations the ligand can assume in this position. Firstly, hydrogen bonds involving the ring carbonyls are expected to be preferred over those formed by the thiol group, while the extra methyl group severely restrains the orientation of the aforementioned ring carbonyls due to clashes between the level 6' serines and the methyl group. Consequently, only two hydrogen bonds can form between thiopental and the residues lining the ion channel pore – one between each carbonyl and an adjacent serine. The carbonyls are positioned at distances of 2.8 Å and 2.7 Å from the closest serines (Fig. 4-C). The distances between the rest of the longer aliphatic chain and the threonines at position 2' range from 4.7 Å to 5.2 Å (Fig. 4-C). It appears that the long aliphatic chain is less flexible facing downwards, as indicated by the observable density in the 2Fo-Fc electron density map. In addition, the anomalous signal of sulphur, located upwards, helped the modelling of the thiopental with its aliphatic chain pointing to the bottom of the pore. The different binding mode of thiopental could be related to the specific rebound current observed upon its washout on oocytes compared to the other barbital derivatives with shorter and simpler aliphatic chains.

Selenocyanobarbital is oriented with its axis of pseudosymmetry parallel to the ion channel, with the side carbonyls of the barbital pyrimidine ring forming hydrogen bonds with serines at level 6' (Fig. 4-D). Selenocyanobarbital was modelled according to a compromise between the experimental 2Fo-Fc density, the selenium anomalous peak and the propensity to form hydrogen bonds. The observed anomalous peak falls in the middle of the pore axis possibly because of the fivefold symmetry of the ion channel rendering barbiturate binding possible in five equivalent different conformations, generated by a rotation of 72º around the C5 pore axis. The observed anomalous signal thus represents an average on the C5 axis of the

individual anomalous signal due to the different possible binding poses within the pore (Fig4-E-F). In the modelled selenocyanobarbital pose, one of the side carbonyls is positioned between two adjacent serine 6' sidechains 2.7 Å and 3.0 Å away, while the distance between the other carbonyl and a third serine residue is 3 Å, thus indicating the formation of three hydrogen bonds in total. The pyrimidine ring nitrogen next to the first carbonyl could potentially weakly interact with the adjacent serine. The second carbonyl is facing downwards close to the threonine ring at level 2', the distance from the closest threonine oxygen being 3.6 Å, indicating the presence of a weak hydogen bond. It could be postulated that the reason the pyrimidine ring of selenocyanobarbital is not found in a similar sideways orientation to that for bromobarbital is because of the length, rigidity and the polar nature of its long terminal tail that is absent in clinically used barbiturates. The terminal carbon of the ethyl tail is oriented toward the isoleucine 9' ring.

DISCUSSION

Previous research, using a photoreactive derivative, has shown the ability of barbiturates to bind to sites within the ion channel pore of the nAChR, a cationic pLGIC [17]. In this study, we solved the first crystal structures of barbiturate binding to this class of receptors, exemplified by the locally-closed GLIC isoform, and we unequivocally locate the barbiturate binding site between residues 2' and 9' in the ion channel (Fig3). The main interactions between barbiturates and the GLIC protein appear to be hydrogen bonds between the barbiturate pyrimidine ring carbonyl groups and the 6' serines. We do observe that the aliphatic tails at position 5 on the ring can further stabilise the binding of the ligand by interacting with 9' isoleucines through van der Waals forces. Interestingly, the presence of thiopental's branched aliphatic tail appears to invert the orientation of the molecule within the pore compared to bromobarbital and selenocyanobarbiturate. This could be caused by the additional steric hindrance of the tail arising from the extra methyl group close to the pyrimidine ring, increasing the probability of a steric clash with the surrounding residues and thus favouring the inverted orientation. This agrees with the previously described structural and functional relationships found in barbiturates with the same empirical formula [16]. For example, barbiturates containing an unbranched position 5 alkyl tail have higher affinity for the ion channel pore (less steric hindrance); however, if a branch exists on the alkyl tail, higher affinities will be observed if the branching is located further away from the pyrimidine ring allowing an upwards orientation with the branch closer to the 9' isoleucines. The characterisation of this binding site presented here thus allows the rationalisation of how modifications to barbiturate structure can alter their functional profile.

In order to predict which state of GLIC is most stabilised by the binding of barbiturates within the ion channel pore, we performed docking calculations similar to the ones described recently [30] on both the closed, open and (modelled) desensitised states of GLIC. Although the structure of this receptor in a desensitised state is currently unknown, the assumption that all pLGICs follow closely related global conformational changes during transitions between different states allowed us to build a putative model of GLIC in the desensitised state, based on the recently published structure of the apparently desensitised $GABA_A$ receptor β3 homomer [22]. Our docking calculations showed that in comparison to the closed pore, in the open state the distances between adjacent 6' serines are increased, giving more conformational freedom to barbiturate binding within this region and allowing deeper penetration into the pore, possibly forming additional interactions with the threonine sidechains at level 2', meanwhile losing the stabilising effect of 9' isoleucines. As a result, the predicted dissociation constants of almost all ligands increase dramatically during the opening and subsequent desensitisation of the receptor (Sup. Fig. 1). The calculated binding modes for thiopental, selenocyanobarbital and bromobarbital in the open state of GLIC were almost identical with their axes of pseudosymmetry perpendicular to that of the protein (Sup. Fig. 2). Interestingly, the calculated binding modes of all barbiturates within the closed pore matched the ones observed by crystallographic methods (Sup. Fig. 3), although thiopental was observed to bind with equal binding energies with its tail found both above and below level 6' serines. Even though the energetics of the docking are not expected to be exact due to a rather crude model for calculating them, these docking calculations qualitatively suggest that barbiturates binding in the ion channel is stronger when the receptor resides in its closed state (Sup. Table). Ligands binding to this site would therefore tend to stabilise this particular state of the receptor, ie, a non-activated, shut state of the channel. Binding studies on barbiturates have shown that derivatives with unbranched position 5 tails bind to the nAChR pore preferentially in its closed state, while others, such as pentobarbital with its branched methylbutyl tail, prefer to bind to the open state, in which the pore

diameter is expanded above 2' residues [16]. This might indicate the presence of a second potential barbiturate binding site within the pore, positioned higher than the one described here, where an increase in the pore diameter would reduce the steric hindrance arising from the presence of extra methyl groups on the barbiturate aliphatic tails. A similar proposal was suggested following photolabelling [17] which identified a putative barbiturate binding site between 9' and 16' in the nAChR channel. However, despite this, no barbiturate binding sites have been crystallographically observed within the open-state GLIC ion channel. Indeed, our own efforts to obtain structures of barbiturates bound to wild-type GLIC in the open-state (at pH 4) were not successful. It is remarkable that, instead, a tight pentagon of water molecules occupies the 6' position in the X-ray structure of open GLIC form, in a manner similar to ice type IX (Sup. Fig. 5) [31]. This water network is important for ion permeation through the hydrophobic barrier in the pore. Moreover, in the open structure, six detergent molecules are lodged within the ion channel pore, possibly precluding ligand binding in this region, especially for low affinity ones.

The present study provides direct experimental evidence for the central ion channel pore of cationic pLGICs being an important site for binding barbiturates to this class of receptor. It is clear that this site may also play a larger role in the overall effects of many other general anaesthetics since smaller volatile general anaesthetics, such as xenon [28] and bromoform [29] have recently been observed to bind to the same site in the locally closed GLIC form (Sup. Fig. 5), while propofol has also been predicted to bind in the central ion channel pore within several states of this receptor [32]. In contrast, the binding site for propofol and desflurane in the open form of GLIC was located by crystallography to an intrasubunit cavity at the top of the TMD α-helical bundle [26], and this was recently validated by chemical labelling experiments [33]. Further studies using mutants of GLIC activated by propofol are currently being pursued in our lab to fully resolve this issue. For barbiturates, since the site described here is found in the closed state of the pore, the inhibitory effects of this class of drugs on cationic pLGICs is readily explained.

This site cannot be responsible for the activation of anionic pLGICs, as i) it blocks the pore and ii) has been shown by photoaffinity labelling experiments that in this case the binding site is located at the interface between subunits in the TMD [34]. However, the inhibition potency of this binding site is likely to be also significant for anionic pLGICs, as it has been shown to mediate alcohol inhibition on GABAA receptor [35]. The identification of the true binding sites of barbiturates onto GABA-A receptors awaits their crystal structure and would be greatly facilitated through the use of molecules such as the ones synthesized for this study thanks to their anomalous signal.

MATERIALS AND METHODS

Synthesis of barbiturate derivatives

Commercially available reagents were used throughout the synthesis without further purification. Analytical thin layer chromatography was performed on Merck 60F-254 precoated silica (0.2 mm) on glass and was revealed by UV light. ^{1}H and ^{13}C NMR spectra were recorded on a Bruker AC 300 at 300 MHz and 75 MHz. The chemical shifts for 1H NMR were given in ppm downfield from tetramethylsilane (TMS) with the solvent resonance as the internal standard. Infrared (IR) spectra were obtained as neat films on Bruker Vector22 spectrophotometer. HRMS (ESI) analysis was performed with a time-of-flight mass spectrometer yielding ion mass/charge (m/z) ratios in atomic mass units. Purity of selenocyanobarbital was determined by reverse phase HPLC using a 150 mm x 2.1 mm (3.5 µm) C18-column: the compound was eluted over 20 min with a gradient from 95% ACN/ 5% (H_2O + 0.1% HCO2H) to 100% (H_2O + 0.1% HCO_2H). Full protocol of synthesis is provided in the supplementary material section.

Electrophysiology

Oocyte preparation. The ovaries were removed from female African *Xenopus laevis* using procedures approved by the UK Animals (Scientific Procedures) Act 1986. Oocytes were separated from the ovaries by using collagenase type 1 (Worthington) dissolved in a Ca^{2+}-free OR2 solution containing: 85 mM NaCl, 5 mM HEPES, 1 mM $MgCl_2$, pH 7.6 adjusted with 1M KOH. After ~3 hrs treatment, defolliculated oocytes were washed 3x with OR2, and then stored in a modified Barth's solution (MBS) containing: 88 mM NaCl, 1 mM KCl, 0.33 mM $Ca(NO_3)_2$, 0.41 mM $CaCl_2$, 0.82 mM $MgSO_4$, 2.4 mM $NaHCO_3$, 10 mM HEPES, pH 7.6 adjusted with 1M NaOH. Oocytes were injected into the nucleus with 27.6 nl of GLIC cDNA and then incubated at 17°C in MBS.

Two-electrode voltage clamp recording. Oocytes expressing GLIC were used the next day after injection. They were superfused with a solution containing: 100 mM NaCl, 2 mM KCl, 2 mM $CaCl_2$, 1

mM $MgCl_2$, 10 mM MES, pH 7.4 adjusted with 1M NaOH. Currents were recorded using two intracellular electrodes filled with 3M KCl, with an Axoclamp 2B amplifier, a Digidata 1322A interface in conjunction with pCLAMP 8 (Molecular Devices). Currents were digitized at 500 Hz and filtered at 50 Hz. Oocytes were voltage-clamped at -60 mV and experiments conducted at room temperature.

Data analysis. Concentration response data were fitted with the Hill equation (below) using Origin ver6 (OriginLab) software:

$$I/ I\ max = 1 / (1 + (EC50 / [A])^{n_H}),$$

where I and Imax represent the current induced by various proton concentrations and the maximal proton-activated current respectively, [A] is the proton concentration, EC_{50} is the concentration producing a half maximal response, and n_H is the Hill coefficient. Data points were normalised to provide a maximal current of 1 in control.

To assess the potency of antagonism, inhibition-concentration relationships for pentobarbital, bromobarbital and thiopental were fitted using:

$$I/I\ max = 1 – [1 / (1 + (IC_{50} / [B])^{n_H})]$$

where I/Imax represents the relative current induced by a pH 5.5 proton concentration in the presence of varying concentrations of barbiturate (B). IC_{50} is the concentration of barbiturate inducing a half-maximal reduction in the agonist current and n_H is the Hill coefficient.

Crystallisation

GLIC was expressed and purified following the previously described protocol [27]. It contained a K33C-L246C mutation, which has been shown to induce the formation of a disulphide bridge between loop 2 of the extracellular domain and the M2-M3 loop of the transmembrane domain. This effectively renders the receptor stable in a locally-closed state, where the pore is trapped in a closed conformation, while the extracellular domain remains in a state similar to that of the open receptor. This so-called LC conformation is also observed in single-point mutations of GLIC such as E243P or H235F [27] as well as other mutations in the M2-M3 loop [36].

Crystals were grown by the use of the vapour-diffusion method in hanging drops at 18°C. The protein samples were supplemented with bromobarbital, selenocyanobarbital or thiopental to give final barbiturate concentrations of 5, 10 and 20 mM, respectively. The samples were then mixed at a 1:1 ratio with the reservoir solution (100 mM NaAc, pH4, 400 mM NaSCN, 3% DMSO, 16% glycerol, 12 – 14.5% PEG 4K). The drops were microseeded with previously obtained crystals of locally-closed GLIC. Small parallelepiped-shaped crystals appeared overnight, reaching their maximum dimensions after one week. Crystals were collected on cryoloops and immediately flash-frozen and stored in liquid nitrogen.

Data collection and processing

The collection of numerous single-crystal datasets took place on beamlines Proxima-I [37] and Proxima-II [38] at Synchrotron Soleil, as well as ID23 [39] and ID29 [40] at the European Synchrotron Radiation Facility. Data collection wavelengths were set at the Kappa peak for each anomalous scatterer present in the ligand of interest. The collected data were integrated with XDS [41] and further scaled with Scala from the CCP4 suite [42]. Similarly to previously described WT and K33C-L246C GLIC, the crystals tested belonged to a C2 spacegroup with one pentamer in the asymmetric unit. To obtain the initial phases of the models the previously described structure of apo-K33C-L246C GLIC was used as a starting model in Refmac5, followed by approximately 60 – 80 cycles of refinement with Buster [43] for each model. NCS restraints were used throughout the refinement process, each cycle of refinement was followed by inspection of the model in the map and manual adjustments were made using Coot [44]. After the initial cycles of refinement, the electron density and anomalous signal maps of the obtained models allowed the identification of ligand binding sites and their subsequent placement within the model structures. Validation of structures was performed by Molprobity [45], while all figures were prepared using Chimera [46].

Modelling and docking

The model of GLIC in a desensitised state was built by standard homology modelling techniques using as a template the only available structure of a desensitised state in the pLGIC family, the β3 homo-pentameric $GABA_A$ receptor[22]. We first optimally positioned Cα coordinates of seven amino-acid long fragments of the open state structure of GLIC onto the structure of the $GABA_A$ receptor. Here optimality refers to finding the positions of the fragments with a minimal local RMSD between the Cαs of the fragments and the Cαs of the β3 subunit. At the end of this process, the trace of a model for the desensitised GLIC is obtained, that

only includes the positions of its Cα atoms. The full backbone was then rebuilt using a sequence of rigid 4-amino-acid-long protein fragments that are concatenated without any degrees of freedom. As described earlier, fragments chosen from a library of representative fragments found in the PDB are fit to the Cα of the trace using a gradual build-up method [47]. The procedure was recently updated and optimized in a Fortran program, Cα2Full, written by one of us (Patrice Koehl), and is freely available from the author upon request. The Cα of the reconstructured backbone differed from the Cα of the trace by less than 0.5 Å. The side chains were then rebuilt using a rotamer library and the mean field optimization method [48] and the whole model was energy-minimised using the CHARMM19 forcefield.

Coordinates of barbiturate derivatives were generated by Buster [43]. Docking of barbiturates within the experimentally observed binding site in both locally-closed, open and modelled desensitised states of GLIC was performed using AutoDock Vina [49] on a Dell PC with an Intel Xeon X5460 quad core processor. The initial conformations of ligands were randomised, and the bonds of the flexible aliphatic barbiturate tails were allowed to freely rotate during the docking calculations. The target structures were the transmembrane domains (residues 193-315 of each subunit) of the locally closed (PDB ID: 3TLV), open (PDB ID:4HFI) and the desensitised model state of GLIC. Before docking, all water and ion atoms, as well as detergent molecules were removed from the structures; all hydrogen atoms were added, partial charges were also included, and nonpolar hydrogens were merged. The docking calculations focused on the experimentally observed barbiturate binding site within the ion pore between residues 2' and 9'. The search volume was a 16 Å-side cube that included all of the aforementioned residues, the sidechain bonds of which were allowed to freely rotate during the calculation. The binding energies calculated by AutoDock Vina were converted to dissociation constants, K_D, in molar units using: $\Delta G = -RT \ln(K_D)$, where R is the gas constant (1.99×10^{-3} kcal K^{-1} mol^{-1}) and T=300K.

Author Contributions

‡These authors contributed equally.

ZF and RR performed and analyzed the X-ray crystallography experiments. DL performed and analyzed the electrophysiology experiments. MD and TS designed and analyzed the experimental data. ED, SDC and DJ designed, performed and analyzed the chemical synthesis of barbiturate derivatives. PK designed and wrote the program to perform GLIC D-state modeling. ZF, RR, TS and MD co-wrote the paper. MD and TS conceived and coordinated the study.

Accession numbers: the GLIC-LC structure coordinates complexed with thiopental, bromobarbital and selenocyanobarbital have been deposited to the Protein Data Bank (PDB) under the accession numbers 5L4E, 5L4H, 5L47 respectively.

ACKNOWLEDGEMENT

We are indebted to Synchrotron SOLEIL (Saint Aubin) and the ESRF (Grenoble) for excellent beamline facilities. We thank Frederic Poitevin for the optimized alignment of GLIC and GABA-R sequences. ZF was funded by the 'Agence Nationate de la Recherche' grant "Pentagate".

The authors declare that they have no conflicts of interest with the contents of this article.

REFERENCES

1. López-Muñoz, F., Ucha-Udabe, R. & Alamo, C. The history of barbiturates a century after their clinical introduction. *Neuropsychiatr. Dis. Treat.* **1,** 329–43 (2005).

2. Lehmann, H. E. & Ban, T. A. Pharmacotherapy of tension and anxiety. *Curr. Psychiatr. Ther.* **12,** 70–80 (1972).

3. López-Muñoz, F. *et al.* History of the discovery and clinical introduction of chlorpromazine. *Ann. Clin. Psychiatry Off. J. Am. Acad. Clin. Psychiatr.* **17,** 113–35 (2005).

4. Nardou, R. *et al.* Phenobarbital but Not Diazepam Reduces AMPA/kainate Receptor Mediated Currents and Exerts Opposite Actions on Initial Seizures in the Neonatal Rat Hippocampus. *Front. Cell. Neurosci.* **5,** 16 (2011).

5. Schober, A., Sokolova, E. & Gingrich, K. J. Pentobarbital inhibition of human recombinant alpha1A P/Q-type voltage-gated calcium channels involves slow, open channel block. *Br. J. Pharmacol.* **161,** 365–83 (2010).

6. Forman, S. A. & Miller, K. W. Anesthetic sites and allosteric mechanisms of action on Cys-loop ligand-gated ion channels. *Can. J. Anaesth. J. Can. Anesthésie* **58,** 191–205 (2011).

7. Zeller, A. *et al.* Inhibitory ligand-gated ion channels as substrates for general anesthetic actions. *Handb. Exp. Pharmacol.* 31–51 (2008). doi:10.1007/978-3-540-74806-9_2

8. Hadipour-Jahromy, M. & Daniels, S. Binary combinations of propofol and barbiturates on human alpha(1) glycine receptors expressed in Xenopus oocytes. *Eur. J. Pharmacol.* **477,** 81–6 (2003).

9. Olsen, R. W. *et al.* Barbiturate and benzodiazepine modulation of GABA receptor binding and function. *Life Sci.* **39,** 1969–76 (1986).

10. Zhou, C., Liu, J. & Chen, X.-D. General anesthesia mediated by effects on ion channels. *World J. Crit. Care Med.* **1,** 80–93 (2012).

11. Jenkins, A., Franks, N. P. & Lieb, W. R. Actions of general anaesthetics on 5-HT3 receptors in N1E-115 neuroblastoma cells. *Br. J. Pharmacol.* **117,** 1507–15 (1996).

12. Yost, C. S. & Dodson, B. A. Inhibition of the nicotinic acetylcholine receptor by barbiturates and by procaine: Do they act at different sites? *Cell. Mol. Neurobiol.* **13,** 159–172 (1993).

13. Löscher, W. & Rogawski, M. A. How theories evolved concerning the mechanism of action of

barbiturates. *Epilepsia* **53 Suppl 8,** 12–25 (2012).

14. Dent, J. A. The evolution of pentameric ligand-gated ion channels. *Adv. Exp. Med. Biol.* **683,** 11–23 (2010).

15. daCosta, C. J. B. & Baenziger, J. E. Gating of pentameric ligand-gated ion channels: structural insights and ambiguities. *Struct. Lond. Engl. 1993* **21,** 1271–83 (2013).

16. Arias, H. R., McCardy, E. A., Gallagher, M. J. & Blanton, M. P. Interaction of barbiturate analogs with the Torpedo californica nicotinic acetylcholine receptor ion channel. *Mol. Pharmacol.* **60,** 497–506 (2001).

17. Hamouda, A. K. *et al.* Identifying barbiturate binding sites in a nicotinic acetylcholine receptor with [3H]allyl m-trifluoromethyldiazirine mephobarbital, a photoreactive barbiturate. *Mol. Pharmacol.* **85,** 735–46 (2014).

18. Oakley, S. *et al.* Recognition of anesthetic barbiturates by a protein binding site: a high resolution structural analysis. *PloS One* **7,** e32070 (2012).

19. Unwin, N. Acetylcholine receptor channel imaged in the open state. *Nature* **373,** 37–43 (1995).

20. Miyazawa, A., Fujiyoshi, Y. & Unwin, N. Structure and gating mechanism of the acetylcholine receptor pore. *Nature* **423,** 949–55 (2003).

21. Weng, Y., Yang, L., Corringer, P.-J. & Sonner, J. M. Anesthetic sensitivity of the Gloeobacter violaceus proton-gated ion channel. *Anesth. Analg.* **110,** 59–63 (2010).

22. Miller, P. S. & Aricescu, A. R. Crystal structure of a human GABAA receptor. *Nature* **512,** 270–5 (2014).

23. Murphy, J. A. *et al.* Fragmentation of nitrone triflates to 9-membered rings. *Org. Lett.* **9,** 3233–3236 (2007).

24. Gingrich, K. J., Burkat, P. M. & Roberts, W. A. Pentobarbital produces activation and block of {alpha}1{beta}2{gamma}2S GABAA receptors in rapidly perfused whole cells and membrane patches: divergent results can be explained by pharmacokinetics. *J. Gen. Physiol.* **133,** 171–188 (2009).

25. Spurny, R. *et al.* Pentameric ligand-gated ion channel ELIC is activated by GABA and modulated by benzodiazepines. *Proc. Natl. Acad. Sci. U. S. A.* **109,** E3028–3034 (2012).

26. Nury, H. *et al.* X-ray structures of general anaesthetics bound to a pentameric ligand-gated ion channel. *Nature* **469,** 428–31 (2011).

27. Prevost, M. S. *et al.* A locally closed conformation of a bacterial pentameric proton-gated ion channel. *Nat. Struct. Mol. Biol.* **19,** 642–9 (2012).

28. Sauguet, L., Fourati, Z., Prangé, T., Delarue, M. & Colloc'h, N. Structural Basis for Xenon Inhibition in a Cationic Pentameric Ligand-Gated Ion Channel. *PLOS ONE* **11,** e0149795 (2016).

29. Laurent, B. *et al.* Sites of Anesthetic Inhibitory Action on a Cationic Ligand-Gated Ion Channel. *Struct. Lond. Engl. 1993* **24,** 595–605 (2016).

30. Franks, N. P. Structural comparisons of ligand-gated ion channels in open, closed, and desensitized states identify a novel propofol-binding site on mammalian γ-aminobutyric acid type A receptors.

Anesthesiology **122,** 787–794 (2015).

31. Sauguet, L. *et al*. Structural basis for ion permeation mechanism in pentameric ligand-gated ion channels. *EMBO J*. **32,** 728–741 (2013).

32. LeBard, D. N., Hénin, J., Eckenhoff, R. G., Klein, M. L. & Brannigan, G. General anesthetics predicted to block the GLIC pore with micromolar affinity. *PLoS Comput. Biol*. **8,** e1002532 (2012).

33. Chiara, D. C. *et al*. Photoaffinity labeling the propofol binding site in GLIC. *Biochemistry (Mosc.)* **53,** 135–142 (2014).

34. Chiara, D. C. *et al*. Specificity of intersubunit general anesthetic-binding sites in the transmembrane domain of the human α1β3γ2 γ-aminobutyric acid type A (GABAA) receptor. *J. Biol. Chem*. **288,** 19343–19357 (2013).

35. Johnson, W. D., Howard, R. J., Trudell, J. R. & Harris, R. A. The TM2 6' position of GABA(A) receptors mediates alcohol inhibition. *J. Pharmacol. Exp. Ther*. **340,** 445–456 (2012).

36. Gonzalez-Gutierrez, G., Cuello, L. G., Nair, S. K. & Grosman, C. Gating of the proton-gated ion channel from Gloeobacter violaceus at pH 4 as revealed by X-ray crystallography. *Proc. Natl. Acad. Sci. U. S. A*. **110,** 18716–18721 (2013).

37. Ascone, I. *et al*. Proxima 1, a New Beamline on the Third Generation SR Source SOLEIL Combining PX and Single-Crystal BioXAS. in *AIP Conference Proceedings* **882,** 872–874 (AIP, 2007).

38. Duran, D. *et al*. PROXIMA 2A – A New Fully Tunable Micro-focus Beamline for Macromolecular Crystallography. *J. Phys. Conf. Ser*. **425,** 012005 (2013).

39. Nurizzo, D. *et al*. The ID23-1 structural biology beamline at the ESRF. *J. Synchrotron Radiat*. **13,** 227–38 (2006).

40. de Sanctis, D. *et al*. ID29: a high-intensity highly automated ESRF beamline for macromolecular crystallography experiments exploiting anomalous scattering. *J. Synchrotron Radiat*. **19,** 455–61 (2012).

41. Kabsch, W. Integration, scaling, space-group assignment and post-refinement. *Acta Crystallogr. D Biol. Crystallogr*. **66,** 133–44 (2010).

42. Winn, M. D. *et al*. Overview of the CCP4 suite and current developments. *Acta Crystallogr. D Biol. Crystallogr*. **67,** 235–42 (2011).

43. Blanc, E. *et al*. Refinement of severely incomplete structures with maximum likelihood in BUSTER-TNT. *Acta Crystallogr. D Biol. Crystallogr*. **60,** 2210–2221 (2004).

44. Emsley, P., Lohkamp, B., Scott, W. G. & Cowtan, K. Features and development of Coot. *Acta Crystallogr. D Biol. Crystallogr*. **66,** 486–501 (2010).

45. Chen, V. B. *et al*. MolProbity: all-atom structure validation for macromolecular crystallography. *Acta Crystallogr. D Biol. Crystallogr*. **66,** 12–21 (2010).

46. Pettersen, E. F. *et al*. UCSF Chimera--a visualization system for exploratory research and analysis. *J. Comput. Chem*. **25,** 1605–12 (2004).

47. Kolodny, R., Koehl, P., Guibas, L. & Levitt, M. Small libraries of protein fragments model native protein structures accurately. *J. Mol. Biol*. **323,** 297–307 (2002).

48. Koehl, P. & Delarue, M. Application of a self-consistent mean field theory to predict protein side-chains conformation and estimate their conformational entropy. *J. Mol. Biol.* **239,** 249–275 (1994).

49. Trott, O. & Olson, A. J. AutoDock Vina: improving the speed and accuracy of docking with a new scoring function, efficient optimization, and multithreading. *J. Comput. Chem.* **31,** 455–61 (2010).

Figures and tables

	Bromobarbital	*Selenocyanobarbital*	*Thiopental*
Data processing			
Wavelength (Å)	0.9192	0.978	1.746
Space group	C2	C2	C2
Cell dimensions			
a, b, c (Å)	177.2 ; 127.9 ; 159.7	181.1 ; 128.1 ; 162.1	182.0 ; 134.6 ; 159.0
α, β, γ (°)	90 ; 101 ; 90	90 ; 103 ; 90	90 ; 102 ; 90
Resolution (Å)	49.56 - 3.30 (3.48 - 3.30)	49.12 - 2.99 (3.15 - 2.99)	49.4 7 - 3.5 (3.69 - 3.50)
Rmerge	9.1 (52.8)	9.5 (65.6)	8.3 (62.3)
I/σ(I)	9.4 (1.9)	9.4 (2.2)	9.4 (1.9)
Completeness (%)	99.4 (99.5)	99.1 (94.3)	99.3 (98.4)
Redundancy	3.1	3.9	3.2
Refinement			
Resolution (Å)	49.13-3.30	47.87-2.99	49.47-3.50
No. reflections	52350	72625	47093
Rwork/Rfree	21.36/23.49	20.9/22.9	22.9/24.9
No. atoms			
Protein	12597	12600	12600
Ligand/ion/detergent	14/05/12	16/5/12	16/5/12
Water	103	115	74
B factors			
Protein	83.51	91.38	127.18
Ligand/ion/detergent	115.43/70.07/65.55	181.77/75.81/72.49	145.87/136.81/82.65
Ramachandran			
favoured (%)	96	96	96
outliers (%)	0	0	0.26
Molprobity score	100th	100th	100th
rms deviations			
Bond lengths (Å)	0.01	0.01	0.01
Bond angles (°)	1.1	1.05	1.11

Table 1. Data collection and refinement statistics.

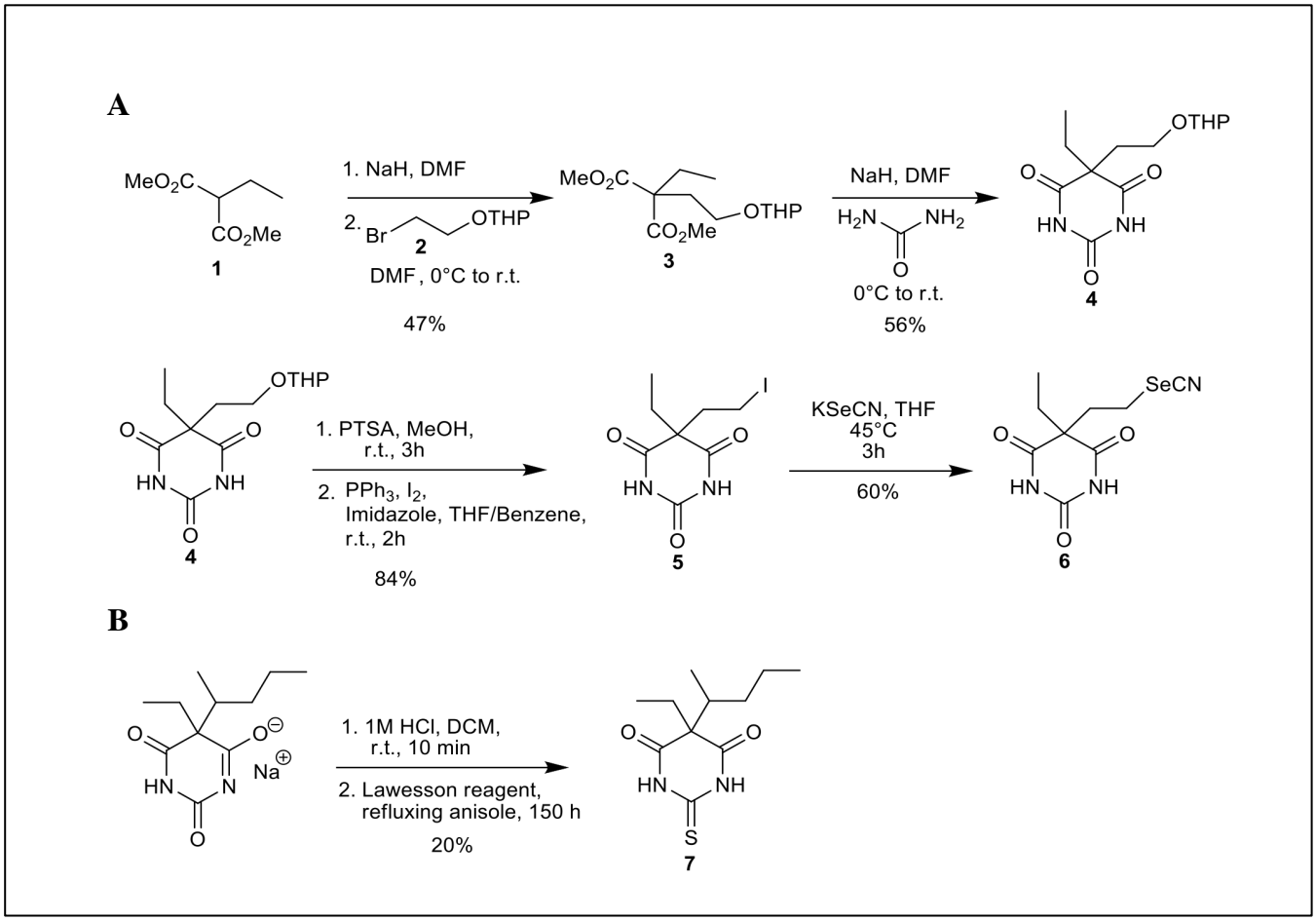

Figure 1. Summary of the different steps in the chemical synthesis of selenocyanobarbital (A) and thiopental (B)

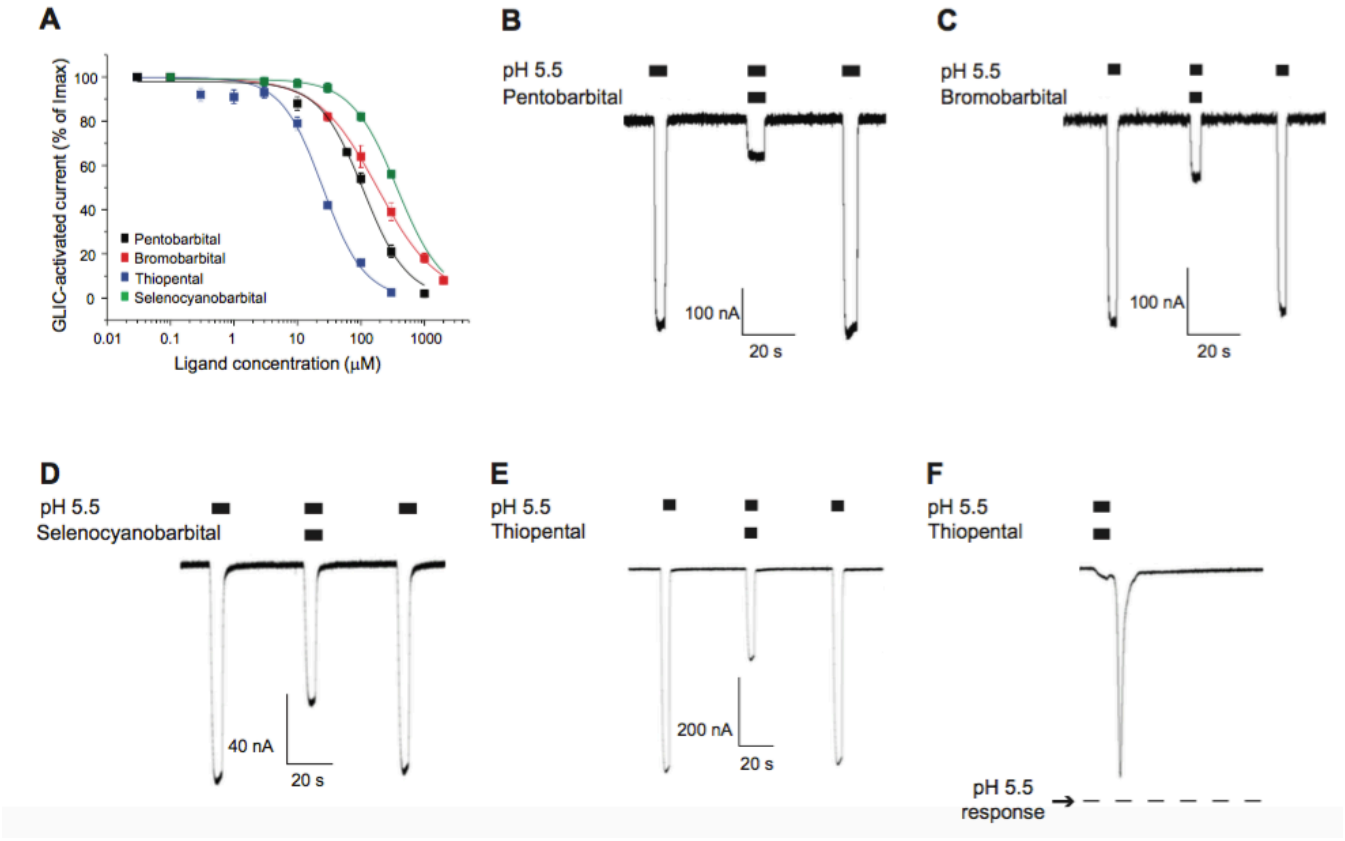

Figure 2. The effect of barbiturates on the proton-induced currents of GLIC expressed in *Xenopus laevis* oocytes. A. Concentration-inhibition curves for pentobarbital, bromobarbital, selenocyanobarbital and thiopental on wild-type GLIC currents activated at pH 5.5. Data points are means ± SEM for n = 5-6 oocytes. B. Representative currents evoked by pH 5.5 showing inhibition of GLIC activation in the presence of (B) 300 μM pentobarbital, (C) 300 μM bromobarbital, (D) 100 μM selenocyanobarbital, or (E) 30 μM thiopental. F. Representative proton current revealing a rebound current after washout of 300 μM thiopental. Dashed line indicates the amplitude of pH 5.5 evoked response in the absence of thiopental.

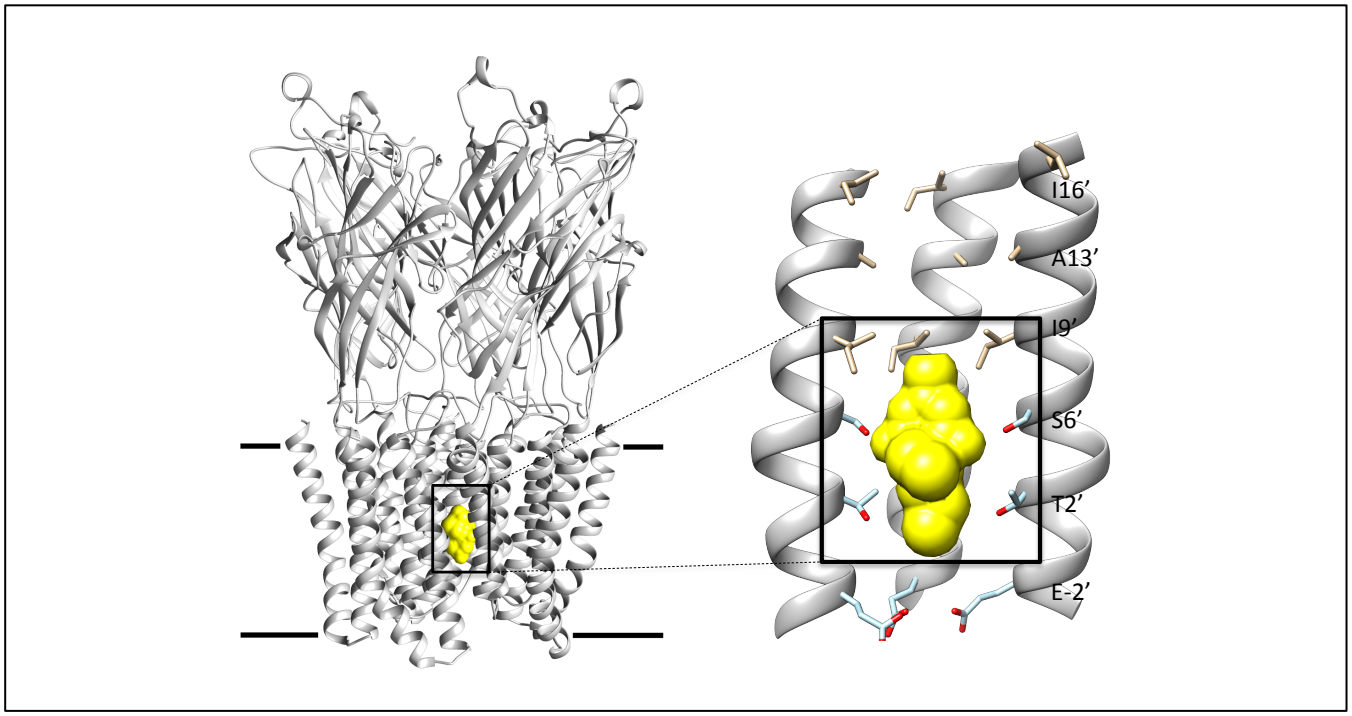

Figure 3: Side view of the full structure of GLIC showing the barbiturate binding site. M2 helices represented as grey ribbons. The box denotes the location of the observed barbiturate binding site (represented in yellow). This site overlaps with the previously described Xenon [28] and bromoform [29] binding sites in GLIC.

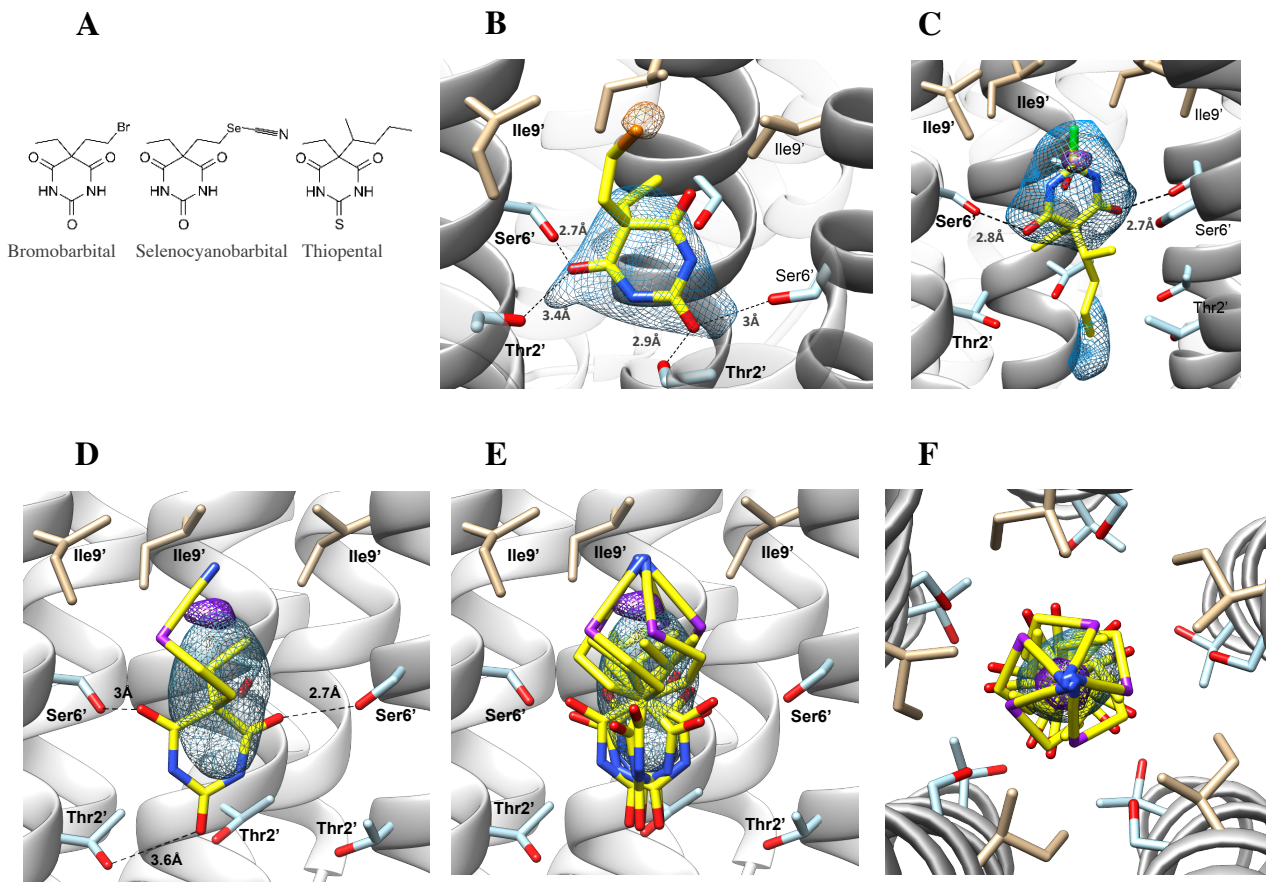

Figure 4. The observed binding sites of different barbiturates within the central ion channel pore of locally closed GLIC. A: Structures of the compounds found to bind the central ion channel pore of GLIC. B: bromobarbital. C: thiopental. D: selenocyanobarbiturate. Note the inversion of thiopental compared to bromo- and selenocyano-barbiturate. Generated symmetric selenocyanobarbiturates : E-side view, F-top view. Residues of interest and ligands shown as sticks, with carbons of hydrophobic residues coloured beige; polar, light blue; ligand, yellow. For heteroatoms: sulphur coloured green; bromine, orange; selenium, purple. Density maps calculated from final refined structures, 2Fo-Fc contoured at 1 σ level and carved around the ligand, while anomalous peaks are shown at 6 σ and 7 σ levels for bromobarbital and both selenocyanobarbiturate and thiopental respectively.

Barbiturates bind in the GLIC ion channel pore and cause inhibition by stabilizing a closed state

Zaineb Fourati, Reinis Reinholds Ruza, Duncan Laverty, Emmanuelle Drège, Sandrine Delarue-Cochin, Delphine Joseph, Patrice Koehl, Trevor Smart and Marc Delarue

J. Biol. Chem. published online December 16, 2016